J. Fluid Mech. (1986), *vol.* 168, *pp.* 291–304
Printed in Great Britain

Experimental study of standing edge waves

By HARRY H. YEH

Department of Civil Engineering, University of Washington,
Seattle, WA 98195, U.S.A.

(Received 3 September 1985 and in revised form 31 December 1985)

Fundamental properties of standing edge waves are investigated experimentally in a physical model with a uniformly and mildly sloping beach with a straight shoreline. Using a unique experimental set-up, quantitative measurements for the detailed nonlinear effects of edge waves are obtained. The experimental results are generally in good agreement with the theoretical predictions (Guza & Bowen 1976*a* and Rockliff 1978) including the offshore profile, dispersion relation, and the outgoing radiated waves generated by the nonlinear interaction of edge waves. The observed behaviour of the excitation process of 'forced' edge waves by the wavemaker can be predicted qualitatively by the inviscid theory, whereas the damping process of 'free' edge waves is governed by the viscous effects, i.e. the theoretical (inviscid) prediction totally underestimates the actual damping phenomenon in the laboratory.

1. Introduction

Edge waves are one of a class of trapped-wave phenomena which can occur near shore owing to wave refraction caused by the variable water depth. In this paper, the standing edge wave is investigated experimentally in a controlled laboratory environment. The primary objective is verification (or identification of shortcomings) of the existing theory (Guza & Bowen 1976*a*; Rockliff 1978), especially nonlinear properties of the standing edge wave.

The first analytical evidence of the existence of edge waves was provided by Stokes (1846). In terms of the departure η of the water surface from its (static) equilibrium position, the Stokes standing edge wave is expressed as

$$\eta = a \sin\beta \exp(-k_m y \cos\beta) \cos k_m x \sin\omega_m t, \tag{1}$$

with the dispersion relation:

$$\omega_m^2 = g k_m \sin\beta, \tag{2}$$

where a is the amplitude of the wave run-up along the beach, β is the angle of the beach slope from the horizontal, x points in the longshore direction, y points offshore, the subscript m denotes the longshore-mode number so that $k_m = m\pi/w$ is fixed by the stationary beach width w. Ursell (1952) demonstrated that the Stokes solution is only the lowest ($n = 0$) of a discrete set of trapped modes with the largest mode number n (a non-negative integer) satisfying $(2n+1)\beta \leqslant \frac{1}{2}\pi$. The dispersion relation for the higher-mode edge wave is given by

$$\omega_m^2 = g k_m \sin(2n+1)\beta. \tag{3}$$

The higher-mode solution also decays asymptotically to zero but having a node(s) in the offshore profile as shown in figure 1 for $n = 0$, 1, and 2 with $\beta = \pi/12$. (The beach slope $\beta = \pi/12$ is used for our experiments discussed in §3.) The shallow-water

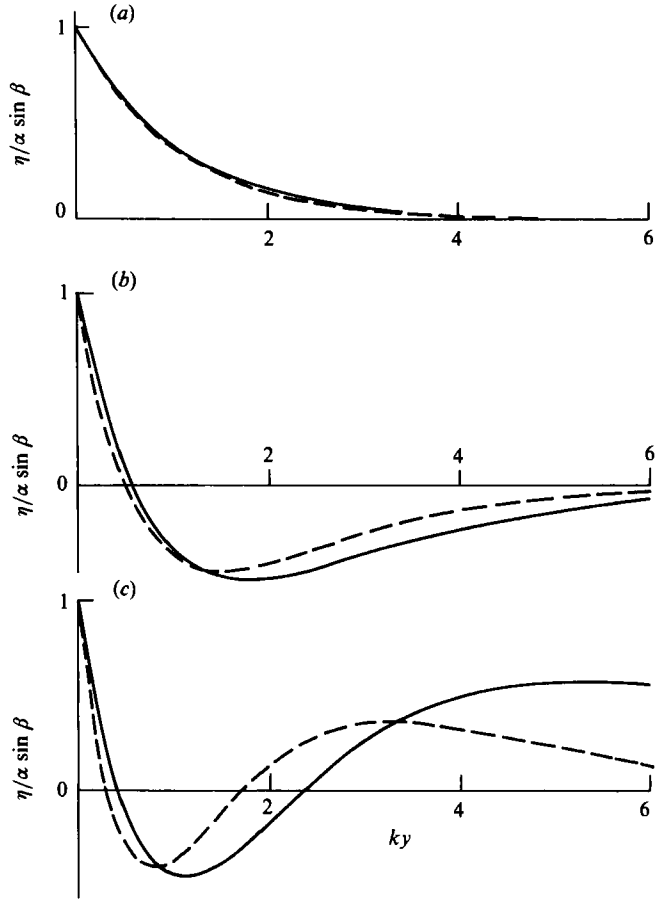

FIGURE 1. Offshore profiles of various edge-wave modes with $\beta = \pi/12$; (*a*) $n = 0$ (Stokes' mode), (*b*) 1, (*c*) 2. ——, full theory; – – – –, shallow-water approximation.

approximation of the higher-mode solution was derived by Eckart (1951). Figure 1 indicates good agreement of the approximation for $n = 0$, but significant discrepancies appear as either n or y increases.

Most of the previous investigations have been focused on the generation mechanism of standing edge waves. Guza & Davis (1974) demonstrated theoretically that standing edge waves can be excited by waves incident from offshore. The nonlinear coupling between the incident–reflected waves of frequency Ω in the cross-shore direction and a small disturbance in the form of an edge wave of subharmonic frequency $\omega = \frac{1}{2}\Omega$ leads to a resonant interaction and growth of the edge wave. The entire evolution process of the edge wave was investigated theoretically by Guza & Bowen (1976*a*), Rockliff (1978) and Minzoni & Whitham (1977). Experimental investigations on the evolution process were made by Guza & Inman (1975), Guza & Bowen (1976*b*), Lin (1981), and Hammack (1982).

The properties of nonlinear standing edge waves themselves were investigated theoretically by Guza & Bowen (1976*a*) and Rockliff (1978). Both investigators showed that nonlinear standing edge waves of the Stokes mode are not completely trapped; wave energy is radiated offshore in the form of outgoing waves of twice the edge-wave frequency. This radiation occurs owing to the formation of resonant triads

among a small disturbance of outgoing waves and two progressive edge waves which combine to form the standing edge wave. The energy radiation offshore was verified qualitatively in the experiments performed by Guza & Bowen (1976*a*) in which a standing edge wave was generated in a small (0.15 m wide, 2 m long, and 0.3 m deep) basin by a wavemaker situated at one of the sidewalls of the beach section. Because of energy leakage, the amplitude of the nonlinear edge wave decays in the absence of an energy source.

In this paper, quantitative experimental measurements for standing edge waves are presented. The edge waves were generated by the experimental apparatus similar to, but with much larger scale than, the apparatus used by Guza & Bowen (1976*a*). Nonlinear properties of edge waves are particularly of interest, e.g. the outgoing radiated waves generated by the nonlinear interaction, the edge-wave profiles, and the excitation and decaying behaviours.

2. Experiments

A series of experiments for standing edge waves was conducted in a wave basin 19.5 m wide, 18.3 m long, and 0.76 m deep. Schematic drawings of plan and elevation views of the basin and beach are shown in figure 2. The slope of the beach was set 15° from the horizontal, $\beta = 15°$. As shown in figure 2, standing edge waves were generated in a small portion of the basin between a reflective wall perpendicular to the shoreline and the wave paddle, 2.48 m from it. This experimental set-up minimizes offshore disturbance, which would influence the standing edge waves; together with the energy absorber (made of rubberized horse hair) on the basin walls, the disturbance incident from offshore is almost eliminated, allowing the examination of the properties of edge waves themselves.

The wavemaker is a wedge-shaped paddle that is hinged offshore and oscillates in the longshore direction about the vertical axis. The linear approximation of the paddle motion for edge waves with exponential offshore decay is analogous to that of 'plunger'- and 'flap'-type wavemakers used for the generation of deep-water waves. The wave paddle is activated by a hydraulic cylinder, and the hydraulic power unit which drives the cylinder is controlled by an electric servo system.

In order to avoid excessive surface contamination of the water, the overflow weir was utilized to skim the water surface continually by providing a slow flow of water into the basin prior to the experiments. The beach surface was wetted prior to the measurements using a small sprinkler system. With this treatment an evenly wet condition in the wave run-up region can be achieved and, more importantly, possible formation of a water–air–beach contact line can be eliminated in an attempt to minimize the influence of surface tension at the locus of the maximum run-up.

Extremely sensitive resistance-type wave gauges were used to measure water-surface variation as a function of time and the data were taken with a sampling rate of 25 Hz. Because the experiments require precise measurements in the large-scale wave basin, each wave gauge was mounted on a remote-controlled gauge positioning system so as to calibrate and position the gauge precisely without disturbing the water. The gauge position can be changed vertically as well as horizontally using the precision of the stepper motors which are controlled by the system outside of the basin. A more detailed discussion of the laboratory apparatus has been presented by Yeh (1983).

Generation of clean standing edge waves requires perfect wave reflection, uniform wave amplitudes between the reflective walls, and a beach width corresponding to edge-wave antinode positions at the reflective walls. These conditions were achieved

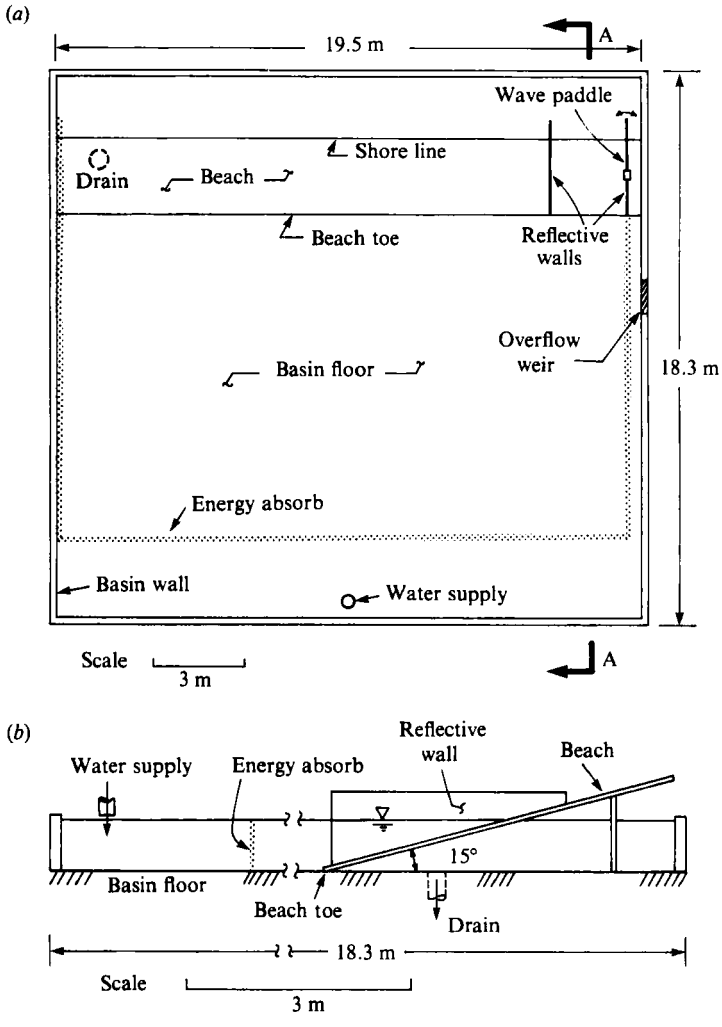

FIGURE 2. Schematic drawings of wave basin; (*a*) plan view, (*b*) section A–A view.

in the experiments which utilized standing edge waves with a longshore-mode number $m = 2$. With this choice, a symmetrical standing edge wave with two longshore nodes is formed between the walls. Wave measurements were taken at various offshore locations along the beach centreline, which corresponds to an edge-wave antinode. In order to extract data regarding nonlinear effects (discussed further in §3) from measured data, the Fourier approximation method was applied for resolving the raw data into fundamental and higher-harmonic components.

3. Results

In this section various aspects of the experimental results are presented and discussed with respect to the theoretical predictions. Included herein are steady-state properties of standing edge waves, the edge-wave excitation process forced by the motion of a sidewall wavemaker, and the decaying process of a free edge wave. In order to investigate the excitation process, we first start the wavemaker with a

prescribed stroke and frequency. The gradually increasing amplitudes of the standing edge wave are measured. The generated edge wave reaches its steady-state condition when the energy input by the wavemaker is balanced by energy leakage offshore due to the radiation and viscous dissipation. In order to study the damping behaviour of free standing edge waves, forcing by the wavemaker is terminated and the time history of amplitude variation from the steady-state condition is measured. We first discuss the steady-state properties followed by the excitation and damping of the standing edge wave.

3.1. *Steady state*

Based on the shallow-water approximation, the solution for the water surface displacement η up to second order (in terms of the nonlinearity parameter ak) was provided by Guza & Bowen (1976*a*) and Rockliff (1978). Extending their solution to that for a mild (small-but-finite) beach slope condition (Yeh 1983) yields

$$\eta = a\sin\beta\{\exp(-ky\cos\beta)\cos kx\sin\omega t - \tfrac{1}{4}ak\exp(-2ky\cos\beta)(1+\cos 2\omega t)\} - \frac{1}{g}\partial_t\phi_1, \quad (4)$$

where ϕ_1 is the second-order velocity potential which represents an outgoing progressive wave of frequency 2ω. The form of ϕ_1 is found in either Guza & Bowen (1976*a*) or Rockliff (1978). The second term in (4) represents the set-down of the mean water level, which oscillates with frequency 2ω. Both Guza & Bowen and Rockliff also derived the dispersion relation of nonlinear standing edge waves. Their results differ slightly in the numerical coefficient for the nonlinear correction; however, since the difference is small, the dispersion relation found by Rockliff,

$$\omega^2 = gk\tan\beta(1+0.094\,a^2k^2), \quad (5)$$

will be used for the comparison with the experimental results presented herein. Note that, owing to the shallow-water approximation, $\tan\beta$ appears in (5) instead of the $\sin\beta$ found in (2).

In order to generate the resonant condition for standing edge waves, the wavemaker is adjusted by trial and error to a frequency that produces the maximum amplitude response with a given stroke of the paddle oscillation. The resulting values of ak are presented in table 1 together with the corresponding paddle strokes S and frequencies ω. Theoretical predictions of the resonant frequencies according to the linear theory (2) and the nonlinear theory (5) are also listed. The experimentally determined resonant frequencies are closer in all cases to those predicted by the linear full water-wave theory than to those of the nonlinear theory based on the shallow-water approximation. This behaviour occurs because the error of the shallow-water approximation is more substantial than the nonlinear effects on the dispersion relation. As seen in table 1, the experimentally determined frequencies are slightly lower than the theoretical values; a similar behaviour was also observed by Guza & Bowen (1976*a*). It should be noted that one of the beach boundaries is the wavemaker so that the finite paddle motion might have some effect on the natural frequencies of standing edge waves. However, strokes of the wavemaker used are too small to explain the discrepancies. A plausible explanation can be made in relation to viscous effects. While the inviscid theory does not predict any energy dissipation, wave energy in a real-fluid environment is always dissipated due to effects of viscosity, which affects both the wave amplitude and phase. A simple model of the viscous effects based on the shallow-water approximation was provided by Guza & Davis (1974). Their

ak	Wave-paddle stroke S at $y = 0$ cm (cm)	ω(rad/s)		
		Measured	Equation (2)	Equation (5)
0.085	1.2	2.52	2.536	2.582
0.146	2.5	2.51	2.536	2.583
0.207	4.1	2.51	2.536	2.586

TABLE 1. Response of standing edge waves

model, however, can only estimate the viscous effects on the amplitude but not on the phase. Here we adopt the model developed by Mei & Liu (1973) who applied the boundary-layer-Poincaré method to small-but-finite amplitude waves and thin laminar-boundary layers; their model provides both the rate of attenuation and the frequency shift due to viscosity. Straightforward application of Mei & Liu's model to the present problem yields

$$\omega = \omega_0 - (1+\mathrm{i})(\tfrac{1}{2}\omega_0)^{\frac{1}{2}}\nu k\left(\frac{1}{\tan\beta}+\frac{1}{kw}\right), \tag{6}$$

where $\omega_0 = (gk\sin\beta)^{\frac{1}{2}}$, ν is the kinematic viscosity, w is the beach width, and $\mathrm{i} = \sqrt{(-1)}$. The first viscous correction involving the term $1/\tan\beta$ represents the dissipation in the beach boundary layer, whereas the correction involving $1/kw$ is due to the boundary layers on the sidewalls. Also note that the imaginary part of (6) is in fact the exponential attenuation rate of amplitude, and the viscous effect on the frequency shift is given by the real part of (6). In the case of $kw \gg \tan\beta$ (i.e. the dissipation in the beach boundary layer is dominant), the imaginary part of (6) reduces the exponential amplitude attenuation rate given by Guza & Davis (1974). For the present condition with $\omega_0 = 2.536$ rad/s, $k = 2.534$ rad/m, $\nu = 1.0\times10^{-6}$ m^2/s, and $w = 2.48$ m, (6) yields $\omega = 2.525$ rad/s. Additional downshift of the observed natural frequency is perhaps due to the viscous effects in the boundary layer at the contaminated free surface. In the fully contaminated state, the surface may be regarded as incompressible so that the surface is horizontally immobilized. Thus its contribution to the dissipation is comparable with that of a solid boundary. Including the comparable downshift of the frequency due to the contaminated surface, the theoretical prediction with the viscous effects is in good agreement with the observed natural frequency.

The maximum amplitude response of edge waves generated by a motion of a sidewall wavemaker was investigated by Rockliff (1978). At the outset of her analysis, she assumed that the amplitude of the paddle motion S is very small, of $O(a^3k^3)$; this assumption implies that the value of ak is proportional to $S^{\frac{1}{3}}$. She incorporated this small forcing term into her slowly varying amplitude equation which is derived by the method of multiple scales; note that her analysis differs from the 'traditional' wavemaker problem in which the complete solution of the boundary-valued problem is sought (e.g. see Wehausen & Laitone 1960, §19). The predicted value of ak based on her theory is presented in figure 3 together with the experimental results. The disagreement is evident; the theoretical value of ak is proportional to $S^{\frac{1}{3}}$, while the measured value of ak appears to be proportional to $S^{\frac{2}{3}}$. The experimental evidence does not support the assumption of the theory, viz. $S \approx O(a^3k^3)$. This discrepancy is important and must be remembered in the theoretical and experimental comparisons for the excitation process discussed in §3.2.

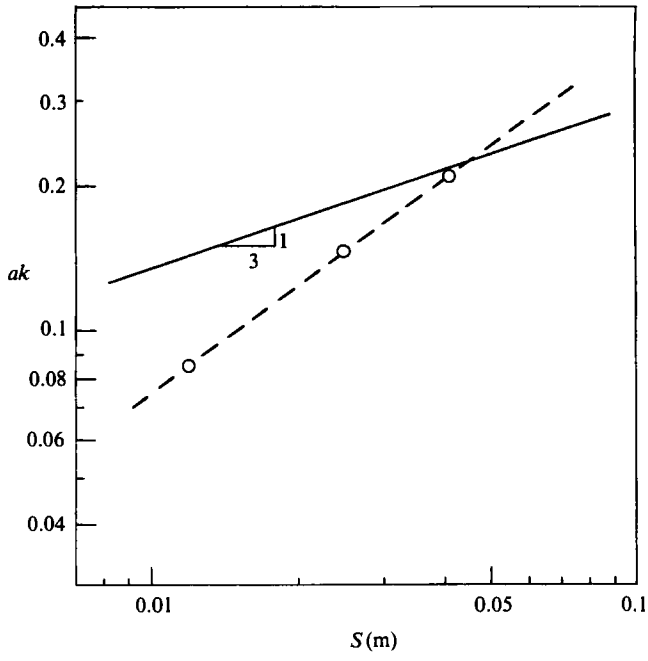

FIGURE 3. Amplitude response of standing edge waves generated by the sidewall wavemaker with paddle stroke S at a shoreline. ○, measured data; ——, theory.

The experimental results for the offshore amplitude profiles of the fundamental-harmonic component are presented in figure 4. Good agreement between the measured data and theory is evident. As ak increases, the offshore decay of the amplitude profile decreases slightly in the offshore region and deviates from the theoretical decay. This may be attributed to the generation of outgoing waves with frequency ω (synchronous to the edge waves) due to the higher-order nonlinear interaction or to direct generation by the wavemaker. (A solution of the wavemaker problem is not known.)

The results of the set-down Δ of the mean water level at $y = 24$ cm ($ky = 0.6$) are presented in table 2 together with the theoretical predictions made by (4). The error bands presented in the table are based on a 95 % confidence limit, assuming the errors to obey a normal distribution (the measurements were repeated 9 times). The experimental results demonstrate the occurrence of the set-down phenomenon; however, the measured values exceed the theoretical values by a factor of approximately 2. The reason for this behaviour is not clear but this trend in the set-down data was also observed experimentally for progressive edge waves (Yeh 1983). Perhaps this discrepancy is related to the run-up/run-down mechanisms which are not modelled by the theory. (The contribution from the existence of a higher-mode edge wave (as discussed next) is too small to explain this discrepancy.)

Offshore amplitude profiles of the second-harmonic component of the standing edge waves are presented in figure 5. Results show two local maxima of the amplitude at $ky \approx 1.0$ and 3.0 with the smallest value at $ky \approx 2.0$ in all three experiments. According to (4) the second-harmonic component consists of the oscillation of the set-down phenomenon as well as the progressive wave radiating offshore; the theoretical amplitude profiles also shown in figure 5 indicate a monotonical decrease in the offshore direction, which contradicts the measured results. A probable cause

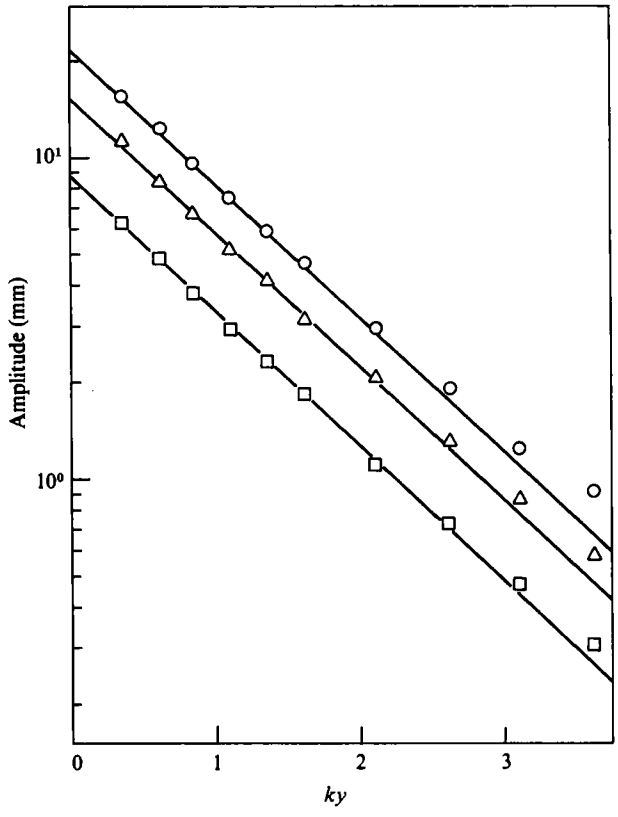

FIGURE 4. Offshore amplitude profiles of the fundamental-harmonic component of standing edge waves. $\omega = 2.51$ rad/s; ○, $ak = 0.207$; Δ, 0.146; □, 0.085; ——, theoretical profile.

	Δ(mm) at $y = 24$ cm		a_r at $y = 84$ cm	Offshore energy flux	
ak	Measured	Theory	(mm)	F_m (N/s)	F_T (N/s)
0.085	0.123 ± 0.049	0.058	0.134	-9.71×10^{-5}	-8.17×10^{-5}
0.146	0.405 ± 0.073	0.175	0.359	-6.97×10^{-4}	-7.28×10^{-4}
0.207	0.619 ± 0.083	0.352	0.765	-3.17×10^{-3}	-2.92×10^{-3}

TABLE 2. Measured and predicted properties of nonlinear standing edge waves

of this contradiction is the occurrence of the higher-mode edge waves. According to Flick & Guza (1980) higher-harmonic waves can be generated directly by a simple sinusoidal motion of a wavemaker. Considering the mode $n = 2$ edge wave, its resonant frequency is found to be $\omega_2 = 4.90$ rad/s, which is close to the second-harmonic frequency, $2\omega = 5.02$ rad/s, of the paddle motion. It is noted that the generation of standing waves in the cross-shore direction is unlikely to occur since the incident waves from offshore were eliminated in our experiments.

In order to identify the propagation characteristics of the radiating outgoing wave, the phase velocities (speed and direction) associated with the second-harmonic component are computed from phase differences measured by multiple wave gauges

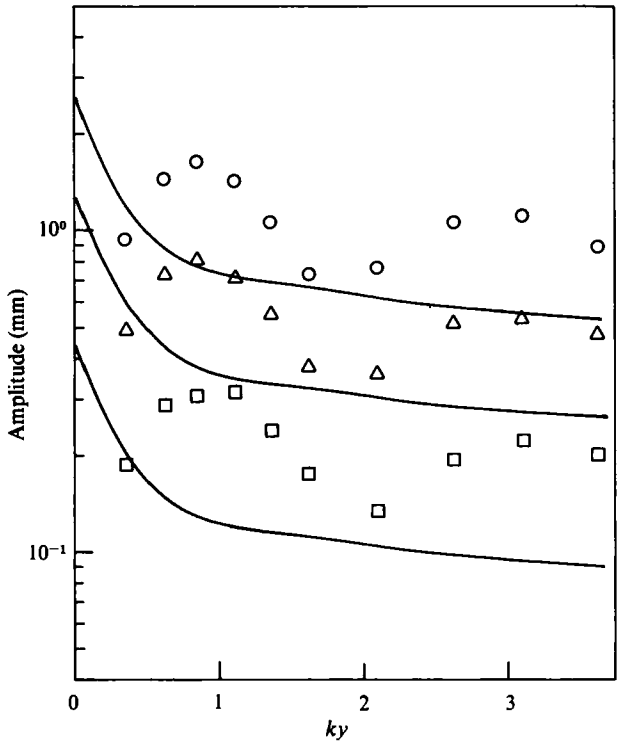

FIGURE 5. Offshore amplitude profiles of the second-harmonic component of standing edge waves. ○, $ak = 0.207$; △, 0.146; □, 0.085; ——, theoretical profile.

and the results are presented in figure 6 as vector diagrams at various offshore locations. The results in figure 6 clearly indicate that the second-harmonic component propagates in the offshore direction. It is noted that the phase velocities shown in the figure are also affected by the oscillating set-down component, and possibly the higher-mode ($n = 2$) edge wave generated by the motion of wavemaker. Perhaps this is why the magnitude and direction of the phase velocities vary slightly.

Guza & Bowen (1976*a*) gave the offshore energy flux associated with the radiated wave, based on the shallow-water approximation, to be

$$F_T = -0.00457\,\rho\pi a^4\omega^3 \tan\beta, \tag{7}$$

where ρ is the density of the fluid. The energy flux in the experiments can be estimated by

$$F_m = -\tfrac{1}{2}C_g\rho g a_r^2, \tag{8}$$

where C_g and a_r are the group velocity and amplitude respectively, of the radiated wave at the offshore location. In order to separate the radiated outgoing wave from the other second-harmonic components, we compute F_m using the measured amplitude a_r at $y = 84$ cm ($ky = 2.1$) because this location corresponds closely to the location of the formation of a node ($ky = 2.4$) for the higher-mode ($n = 2$) edge wave as shown in figure 1. Furthermore, it is far enough offshore for the oscillating set-down effect to be negligible. The group velocity C_g is estimated roughly using the linear dispersion relation of waves in constant depth; since the beach slope is mild, the constant-depth approximation for the group velocity should give a reasonably good estimate. The measured results are presented in table 2 together with the theoretical

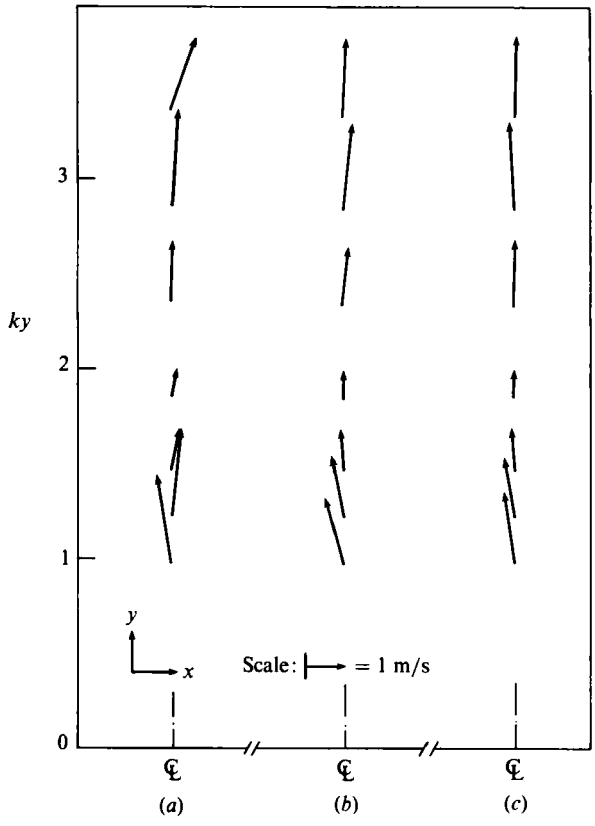

FIGURE 6. Phase speed and direction offshore along beach centreline for the second-harmonic component of standing edge waves; (*a*) $ak = 0.085$; (*b*) 0.146; (*c*) 0.207.

prediction made by (7). Considering the accuracy of the small-amplitude measurements at $y = 84$ cm and the basis of the estimates for C_g, the experimental results are in excellent agreement with the theoretical results in all three cases. This excellent agreement, in turn, supports our conjecture of the existence of higher-mode ($n = 2$) standing edge waves with the second-harmonic frequency.

3.2. *Excitation*

Based on the shallow-water approximation, Rockliff (1978) considered the excitation of edge waves with the motion of a sidewall wavemaker. According to Rockliff, the amplitude of edge waves increases linearly during the initial stage of excitation. As the edge-wave amplitude grows, its finite amplitude leads to the development of processes which limit further growth. Such processes are the generation of the outgoing radiated waves which leak energy to the offshore, the retuning of the natural frequency by the finite-amplitude effect as indicated by (5), and, in a real-fluid environment (but not in Rockliff's model), energy dissipation due to fluid viscosity. Hence, the edge wave excited by the wavemaker eventually reaches its equilibrium condition. However, as discussed in §3.1, the equilibrium condition, i.e. the maximum steady-state amplitude, cannot be predicted correctly by Rockliff's theory. Hence, it is not clear that Rockliff's model is appropriate to use to test the experimental results, or vice versa.

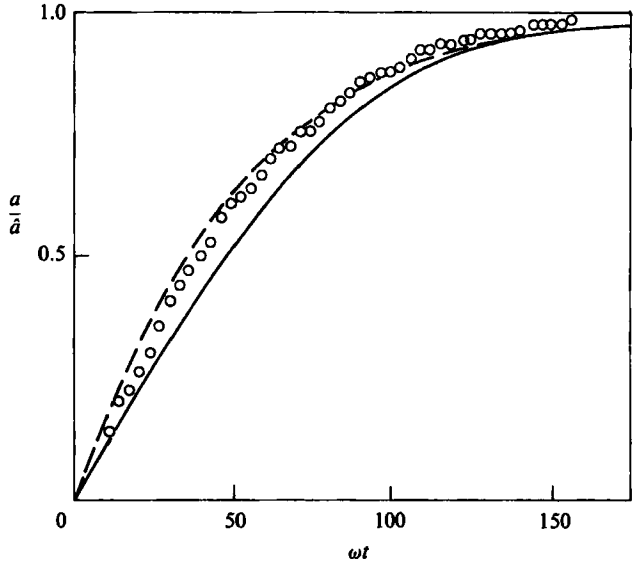

FIGURE 7. Amplitude excitation of forced standing edge waves by the sidewall wavemaker; $ak = 0.207$; ○, measured data; ——, theory; – – – –, modified theory.

The measured time history of the excited edge-wave amplitude is shown in figure 7 together with Rockliff's theoretical (inviscid) prediction and the modified theoretical growth accounting for viscous effects. The modification is based on the lowest-order (linear) dissipation effects with the measured decay rate of free edge waves presented in §3.3. In order to extract the qualitative behaviour of the growth, amplitudes are normalized by their maximum steady-state values $\hat{a}$; the values of $\hat{a}k$ are 0.207 for the experiment, 0.217 for the inviscid theory, and 0.129 for the modified theory. It is emphasized that good agreement of the measured value of $\hat{a}k$ with the theoretical (inviscid) prediction is misleading since the theory cannot predict the equilibrium amplitudes generated with other than this particular wave-paddle stroke. Nonetheless, reasonably good agreement for the qualitative behaviour of the excitation process is evident in figure 7. In spite of the discrepancy in the forcing term in the theory (as discussed in §3.1), the measured growth appears to be in excellent agreement with the modified theory. The viscous effects existing in the experimental result, as well as incorporated into the model, simply reduce the equilibrium wave amplitude but do not significantly influence the behaviour of the excitation process.

3.3. *Damping of free standing edge waves*

Because of energy leakage, the amplitude of the nonlinear standing edge wave decays in the absence of an energy source. Guza & Bowen (1976*a*) derived the evolution equation for amplitude decay, and its solution in terms of the run-up amplitude can be found to be

$$a(t) = \{0.115\omega k^2 t + a(0)^{-2}\}^{-\frac{1}{2}}, \tag{9}$$

where $a(0)$ is the initial run-up amplitude at $t = 0$.

In order to study the damping behaviour of free standing edge waves, the steady-state condition was first established by the wavemaker. Then, forcing by the wavemaker was terminated and the time history of amplitude variation for the free wave was measured at $y = 24$ cm ($ky = 0.60$). The measured time history with the

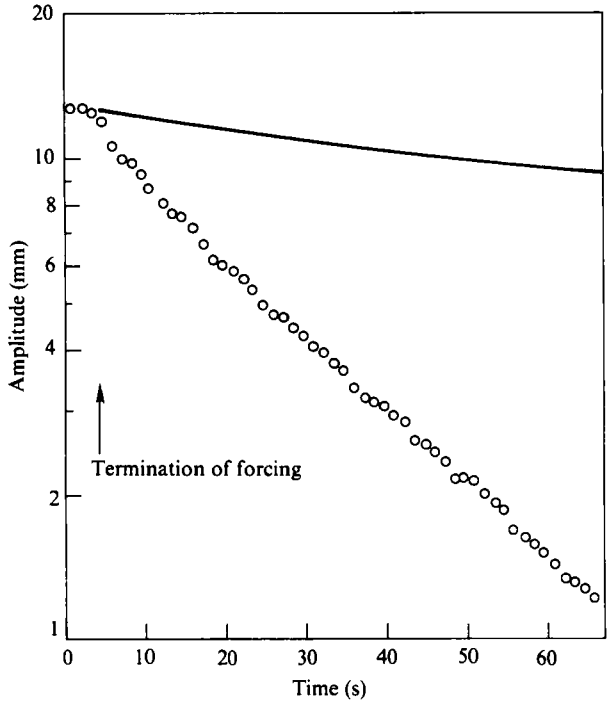

FIGURE 8. Amplitude damping of free standing edge waves in the absence of energy source; $ak = 0.207$; ○, measured data; ——, theory by (9).

initial value of $ak = 0.207$ is presented in figure 8 together with the prediction made by the inviscid nonlinear theory of (9). It is evident that the theoretical prediction significantly underestimates the observed damping. Furthermore, the observed damping appears to be exponential. Apparently, viscous dissipation totally dominates the damping behaviour in the experiment although careful examination of the data in figure 8 reveals that the exponential damping rate is gradually decreased during the process owing to decreasing energy leakage by the nonlinear effect in the initial stage.

The damping of free standing edge waves was previously observed by Lin (1981). (Lin's experimental results are also shown in Hammack 1982.) In his results the damping behaviour appears to be different from that of the present result. According to his data, amplitudes of free standing edge waves decayed slowly in the early stage of the process. The damping rate gradually increased and asymptotically reached exponential. It is noted that in his experiments the standing edge wave was initially generated indirectly by waves normally incident onto the beach from offshore. Thus termination of the wavemaker does not immediately eliminate a forcing mechanism until incident and reflected waves disappear. Furthermore, the complex demodulation technique used in his data analysis involves the band-pass filtering process so that any abrupt change of the wave behaviour is smoothed out and numerically biased. These two factors might be responsible for Lin's observation of the more gradual transition to an exponential damping state.

The theoretical viscous-damping rate can be obtained by (6). The e-folding time of the theoretical damping can be found to be 91 s, whereas the e-folding time of the observed damping in figure 8 is 28 s; the observed exponential damping rate

exceeds the theoretical rate by a factor of approximately 3. As discussed in §3.1, the discrepancy between the theoretical and measured damping rates can be partly attributed to the existence of a surface film produced by contamination. Other possible factors for this discrepancy may be related to the wave run-up and run-down processes on the beach. For example, formation of an air–water–beach contact line can create water-surface curvatures with small radii so that energy transfer to capillary waves may occur there. Also the flow domain near and at the shoreline must be saturated by the boundary layers, and the energy-dissipation mechanism at the saturated boundary layer is not known but may contribute to the additional dissipation.

4. Conclusions

Basic properties of standing edge waves were investigated experimentally using a wave basin larger than that used in a similar experimental study by Guza & Bowen (1976*a*). Taking this scale advantage, detailed and quantitative measurements for the nonlinear effects of edge waves are taken in a carefully controlled environment. Based on the experiments described herein, the following conclusions can be drawn regarding standing edge waves.

(i) The dispersion relation for edge waves is verified in the experiments by modifying the inviscid theory to account for the viscous effects existing in a real-fluid environment.

(ii) The amplitude of edge waves generated by the motion of the sidewall wavemaker with stroke S is found to be proportional to $S^{\frac{4}{3}}$. This experimental evidence contradicts the assumption involved in the theory by Rockliff (1978).

(iii) The amplitude of the standing edge wave decays exponentially offshore at the same rate as predicted by the theory.

(iv) The set-down phenomenon of the mean water level occurs; the measured values, however, exceed the theoretical magnitude by a factor of approximately 2.

(v) The theory can predict not only the occurrence of outgoing radiated waves in the experiments, but also their quantitative magnitude, direction, and the outgoing energy flux.

(vi) In the present experimental conditions, the higher-mode ($n = 2$) standing edge waves may be generated at twice the frequency of the paddle motion.

(vii) In spite of the uncertainty of the validity of the theory (Rockliff 1978), the qualitative behaviour of the excitation process is not significantly influenced by the viscous effects or the magnitude of forcing by the wavemaker motion.

(viii) The theoretical prediction of the damping of free standing edge waves, based on energy leakage offshore, totally underestimates the actual damping phenomenon in the laboratory where the process is governed by dissipation effects.

I am indebted to Professor J. L. Hammack for suggesting this topic. The work for the paper was supported in part by the University of California, Berkeley, and by the National Science Foundation Grant No. ENG-781/697. The Graduate School of the University of Washington also provided support for the preparation of the paper.

REFERENCES

ECKART, C. 1951 Surface waves on water of variable depth. *Wave Rep. No.* 100, Scripps Inst. of Oceanography, University of California.

FLICK, R. E. & GUZA, R. T. 1980 Paddle generated waves in laboratory channels. *Proc. Am. Soc. Civ. Engrs* **106** (WW1) 79–97.

GUZA, R. T. & BOWEN, A. J. 1976*a* Finite amplitude edge waves. *J. Mar. Res.* **34**, 269–293.

GUZA, R. T. & BOWEN, A. J. 1976*b* Resonant interactions for waves breaking on a beach. In *Proc. 15th Coastal Engng Conf. ASCE*, pp. 560–579.

GUZA, R. T. & DAVIS, R. E. 1974 Excitation of edge waves by waves incident on a beach. *J. Geophys. Res.* **79**, 1285–1291.

GUZA, R. T. & INMAN, D. L. 1975 Edge waves and beach cusps. *J. Geophys. Res.* **80**, 2997–3012.

HAMMACK, J. L. 1982 Small-scale ocean waves. In *Topics In Ocean Physics*, pp. 278–311. Soc. Italiana de Fisica.

LIN, N. K. 1981 Excitation of Edge Waves. Ph.D. thesis, University of California, Berkeley.

MEI, C. C. & LIU, L. F. 1973 The damping of surface gravity waves in a bounded liquid. *J. Fluid Mech.* **59**, 239–256.

MINZONI, A. A. & WHITHAM, G. B. 1977 On the excitation of edge waves on beaches. *J. Fluid Mech.* **79**, 273–287.

ROCKLIFF, N. 1978 Finite amplitude effects in free and forced edge waves. *Proc. Camb. Phil. Soc.* **83**, 463–479.

STOKES, G. G. 1846 Report on recent research in hydrodynamics. In *Rep. 16th Meeting Brit. Assoc. Adv. Sci.*, pp. 1–20. (Also in *Math. Physics Paper 1* (1880), pp. 157–187. Cambridge.)

URSELL, F. 1952 Edge waves on a sloping beach. *Proc. R. Soc. Lond.* A **214**, 79–97.

WEHAUSEN, J. V. & LAITONE, E. V. 1960 Surface waves. In *Handbook der Physik* (ed. W. Flügge), vol. 9, 446–778. Springer.

YEH, H. 1983 Nonlinear edge waves. *Rep. No.* UCB/HEL-83/04, University of California, Berkeley.